10-2024

# A LiDAR-driven Pruning Algorithm to Delineate Canopy Drainage Areas of Stemflow and Throughfall Drip Points

Collin Wischmeyer

Travis E. Swanson

Kevin E. Mueller

Nicholas R. Lewis

Jillian Bastock

*See next page for additional authors*

## Authors

Collin Wischmeyer, Travis E. Swanson, Kevin E. Mueller, Nicholas R. Lewis, Jillian Bastock, and John T. Van Stan II

Received: 29 November 2023 | Accepted: 1 June 2024

DOI: 10.1111/2041-210X.14378

Methods in Ecology and Evolution

RESEARCH ARTICLE

# A LiDAR-driven pruning algorithm to delineate canopy drainage areas of stemflow and throughfall drip points

Collin Wischmeyer[1] | Travis E. Swanson[2] | Kevin E. Mueller[1] | Nicholas R. Lewis[1] | Jillian Bastock[1] | John T. Van Stan II[1,3]

[1]Department of Biological, Geological, and Environmental Sciences, Cleveland State University, Cleveland, Ohio, USA

[2]The Water Institute of the Gulf, Baton Rouge, Louisiana, USA

[3]Department of Mechanical Engineering, Cleveland State University, Cleveland, Ohio, USA

**Correspondence**
John T. Van Stan II
Email: j.vanstan@csuohio.edu

**Funding information**
Division of Environmental Biology, Grant/Award Number: 2213623

**Handling Editor:** Carlos Alberto Alberto Silva

## Abstract

1. Precipitation channelled down tree stems (stemflow) or into drip points of 'throughfall' beneath trees results in spatially concentrated inputs of water and chemicals to the ground. Currently, these flows are poorly characterised due to uncertainties about which branches redirect rainfall to stemflow or throughfall drip points.
2. We introduce a graph theoretic algorithm that 'prunes' quantitative structural models of trees (derived from terrestrial LiDAR) to identify branches contributing to stemflow and those contributing to throughfall drip points. To demonstrate the method's utility, we analysed two trees with similar canopy sizes but contrasting canopy architecture and rainfall partitioning behaviours.
3. For both trees, the branch 'watershed' area contributing to stemflow (under conditions assumed to represent moderate precipitation intensity) was found to be only half of the total ground area covered by the canopy. The study also revealed significant variations between trees in the number and median contribution areas of modelled throughfall drip points (69 vs. 94 drip points tree$^{-1}$, with contributing projected areas of 28.6 vs. 7.8 m$^2$ tree$^{-1}$, respectively). Branch diameter, surface area, volumes and woody area index of components contributing to stemflow and throughfall drip points may play a role in the trees' differing rainfall partitioning behaviours.
4. Our pruning algorithm, enabled by the proliferation of LiDAR observations of canopy structure, promises to enhance studies of canopy hydrology. It offers a novel approach to refine our understanding of how trees interact with rainfall, thereby broadening the utility of existing LiDAR data in environmental research.

**KEYWORDS**
ecohydrology, forest hydrology, graph theory, precipitation partitioning, terrestrial LiDAR, urban forestry

## 1 | INTRODUCTION

Setting the boundaries of a research system is crucial, especially when studying environmental systems. This is evident in the watershed boundary concept, a key example, which has been integral to water-related environmental research for centuries (Dalton, 1802). By demarcating the land area over which precipitation ultimately drains to the stream discharge point, the watershed boundary concept enabled significant advances in our understanding of streamflow and its chemical, physical and biological characteristics (Druschke, 2018; Peel & McMahon, 2020; Smith, 2019). Remote sensing has played pivotal roles in delineating and monitoring ecohydrological boundaries across scales, from boundaries of watersheds (Fortin et al., 2001) and local-scale wetlands that are critical to the study of hydrology and ecosystem science (Jeziorska, 2019; Zhang et al., 2022), to boundaries of individual tree canopies in forests that are critical to the study of forest ecology and management (Qin et al., 2022; Reitberger et al., 2009). Since the precise delineation of a system's water-capturing boundaries has broadly aided to advance ecological research, surely remaining uncertainties in such boundaries can hinder the refinement and expansion of our understanding across numerous disciplines. Investigations without well-constrained boundaries are prone to encompassing an excessive array of related variables and, thereby, risk concluding that variability in an observed system process is governed by an exceptionally complex interplay among these variables. This fundamental principle dates back to the philosophical inquiries of Aristotle (in *Metaphysics*, Book V, 1022a4–5) and the methodological rigour suggested by Euclid (in *Elements*, §I, def. 13) that laid the early groundwork for what would evolve into systems theory (Von Bertalanffy, 1950). We posit that the understanding of water movement via throughfall and stemflow through tree canopies (Sadeghi et al., 2020; Stubbins et al., 2020), the start of the rainfall-to-runoff pathway in forests, is limited by unclear boundaries.

Throughfall is the fraction of rainfall that reaches the ground through gaps in the canopy or by dripping from the surfaces of the canopy, whereas stemflow is the portion of precipitation that adheres to the plant canopy and ultimately drains down the branches to the stem, then to the ground. A portion of precipitation does not reach the ground, being stored on, or evaporated from, canopy elements—this is referred to as interception (Coenders-Gerrits et al., 2020; Klamerus-Iwan et al., 2020). Throughfall and stemflow create significant spatiotemporal variability in precipitation inputs to the surface (Fischer-Bedtke et al., 2023; Voss et al., 2016; Zimmermann et al., 2009). This variability is influenced by factors like plant species identity, canopy structure, and rainfall attributes (Van Stan, Hildebrandt, et al., 2020). For example, localised throughfall inputs (at the meter scale) generally range from 'dry' spots, which receive very little precipitation below the canopy, to areas below branch 'drip points' that can receive up to tenfold the amount of open precipitation (Cavelier et al., 1997; Shuttleworth, 1989; Zimmermann et al., 2009). Similarly, stemflow from different trees can vary greatly, from <1% to >30% of precipitation in a single storm (Van Stan & Gordon, 2018).

Strong mechanistic inferences into the drivers of this spatiotemporal variability in stemflow and throughfall have been elusive; however, this understanding is relevant to a host of environmental processes and functions, for example, plant nutrient uptake and leaching (Aubrey, 2020), litter decomposition (Qualls, 2020), surface runoff (Gotsch et al., 2018; Ji et al., 2022), soil erosion (Dunkerley, 2020), subsurface flows (Friesen, 2020) and plant microbiome composition and function (Van Stan, Morris, et al., 2020). Nonetheless, when reviews scrutinise the factors impacting these fluxes—which are numerous and growing—they typically draw attention to the frequently conflicting findings between studies (Levia & Frost, 2006; Levia & Germer, 2015; Parker, 1983). These conflicting findings are then interpreted to bolster the current theory on throughfall and stemflow dynamics, despite its predictive limitations, by underscoring the 'complex relationships' that exist among these numerous factors and the variability of throughfall or stemflow (Carlyle-Moses et al., 2018; Levia & Frost, 2006; Levia & Germer, 2015; Van Stan et al., 2014; Zhang et al., 2020). However, the bulk of these studies focus on the use of observational, regression-based analyses (potentially overburdened by these many variables). We propose a ground up approach and ask: can we reduce the nebulous 'complexity' underlying these idiosyncratic results? Could it be that the current theoretical understanding of the factors controlling throughfall and stemflow is missing something crucial: appropriate boundaries?

New opportunities to delineate the boundaries of canopy drainage areas are made possible by recent advancements in remote sensing, particularly terrestrial LiDAR observations that inform canopy structural models (Atkins et al., 2018; Brede et al., 2022; Hackenberg et al., 2021; Lau et al., 2018). These tools excel at reconstructing branches and forming architectural networks. As stemflow and concentrated throughfall (drip points) largely result from branch-mediated rainfall capture and redistribution (Van Stan et al., 2021), using these remote sensing techniques can help identify branch network components specific to stemflow and drip points. In turn, delineation of these branch 'watersheds' will allow acquisition of new knowledge about characteristics of both rainfall and the canopies that mediate flows of rainfall through trees. Current studies often assume the entire canopy's area (or volume) as their system's boundary (see reviews by Levia et al., 2011; Levia & Germer, 2015; Sadeghi et al., 2020). While this might be valid for continuous forest cover, it can obscure the physical interactions between rainwater and canopy structures that ultimately determine the pathways and volumes of throughfall and stemflow. Studies focused on smaller scale interactions (e.g. sub-canopy scale) often link throughfall's area to the collector's area (Levia et al., 2011; Sadeghi et al., 2020, and references therein), while an individual tree's stemflow area is equated to the 2D projected canopy area (Levia & Germer, 2015; Van Stan & Pinos, 2023, and references therein). With rainwater being directed in different ways by branches of various dimensions and angles, these assumptions about the relevant boundaries may be erroneous often enough for concern. Throughfall, therefore, may come from as small an area as a canopy gap or a vast branch-leaf

network (Zimmermann et al., 2009). Likewise, a single tree's stemflow might originate from a few branches in one instance but from most of the canopy in another (Herwitz, 1986).

Ecohydrological research would greatly benefit from advanced remote sensing techniques that can quantitatively identify canopy drainage areas for hotspots of rainfall flow out of tree canopies, including stemflow and throughfall drip points. This study introduces a new approach that employs graph-based models to analyse quantitative structural models (QSMs) of tree canopies that are derived from terrestrial lidar scans. Through this remote sensing method, we aim to identify the boundaries of branch systems that contribute to rainwater drainage, specifically focusing on stemflow and throughfall drip points in isolated trees. Due to the rapidly growing collection of terrestrial lidar data in forested systems (Calders et al., 2020; Dassot et al., 2011; Disney, 2019) and the nascency of tools for analysing trees in lidar point clouds, there is widespread potential for our QSM-pruning approach to advance hydrology and its integration into other disciplines, like forest ecology and management.

## 2 | METHODS FOR DELINEATING THROUGHFALL AND STEMFLOW CANOPY DRAINAGE AREAS

### 2.1 | Terrestrial lidar scanning and quantitative structural modelling

Quantitative structural models of two trees, representing different stemflow production (low and high), were derived using terrestrial lidar scanning in the winter leafless season at Secrest Arboretum, Wooster OH, USA (40°46′41.9″ N 81°55′06.2″ W, 311 m a.s.l.). Trees studied were *Celtis occidentalis* L. (common hackberry) and *Ulmus americana* L. (American elm). Both trees were planted in a demonstration plot of potential 'shade trees', with sufficient gaps between plantings that both focal tree canopies were isolated from their neighbours, with no branch overlap. They were selected due to their similar size (Table 1) but visually distinct branch architecture (see QSMs in Figure 1) and stemflow production (Lewis et al., 2022). Across 34 rain events, *U. americana* produced 851 L of stemflow compared to 102 L by *C. occidentalis*. The *C. occidentalis* tree only produced stemflow during storms >6.5 mm event$^{-1}$; while the *U. americana* tree produced stemflow during storms as small as 1.4 mm event$^{-1}$.

3D point clouds of each tree were obtained with a BLK360 scanner (Leica Geosystems, USA). With its range of 0.5–45 m and measurement rate up to 680,000 points s$^{-1}$, three scans were taken for each tree from locations oriented ~120° from each other, at 6–8 m from the stem. Care was taken to ensure that scans were performed in orientations intended to maximise branch exposure to the scanner and during optimal weather conditions to minimise occlusion of features due to noise or movement generated by wind. All scans were performed using the 'high density' setting (5 mm point spacing at 10 m range scan$^{-1}$). Scan co-registration was done in Leica's Cyclone Register 360 software, resulting in overall co-registration errors of 0.005–0.011 m. Co-registered point clouds for each study tree were manually trimmed in this software, removing points of surrounding objects to isolate points representing the tree.

The trimmed point clouds were imported into CompuTree 5.0 (http://computree.onf.fr/) and analysed using the SimpleForest plugin (https://gitlab.com/SimpleForest/computree) to develop QSMs (Hackenberg et al., 2021). Resulting tree QSMs contain aggregate tree attributes, with each branch 'cylinder' containing details like: (a) grouping variables based on allometric structures, for example segment id, branch id and branch order; (b) relationship indicators between cylinders, for example parent–child branches, parent segment and parent branch; (c) 3D spatial coordinates (x, y, z) of cylinder poles; and (d) physical attributes of the cylinders, for example length, radius and volume. For further QSM details, see Hackenberg et al. (2021). The diameter range for the most distal branch orders in the QSMs, 2.5–4.9 mm (mean = 3.8 mm), compared favourably to branches physically measured for a separate project 2.6–5.9 mm (mean = 4.1 mm).

### 2.2 | Derivation of graph models from QSMs

Our methodology applies techniques from graph theory, a concept rooted in 150 years of mathematical study (Cayley, 1857), to elucidate hydrologic connectivity in tree canopy QSMs. Graph modelling applications in geosciences are diverse (Phillips et al., 2015) and, as

**TABLE 1** Comparison of traits for each study tree estimated from the lidar-derived quantitative structural models for the total canopy and stemflow-contributing branch components (i.e. the stemflow watershed).

| | Total canopy | | Stemflow watershed | |
|---|---|---|---|---|
| **Traits (units)** | ***C. occidentalis*** | ***U. americana*** | ***C. occidentalis*** | ***U. americana*** |
| DBH (cm) | 0.31 | 0.29 | 0.31 | 0.29 |
| Height (m) | 12.3 | 12.2 | 12.3 | 12.2 |
| Projected canopy area ($m^2$) | 89.3 | 82.3 | 49.0 | 44.3 |
| Projected branch area ($m^2$) | 42.9 | 21.4 | 14.4 | 7.1 |
| Woody area index ($m^2\,m^{-2}$) | 0.48 | 0.26 | 0.29 | 0.17 |
| Branch surface area (SA, $m^2$) | 303.8 | 120.8 | 96.1 | 52.0 |
| Branch volume (*V*, $m^3$) | 4.7 | 1.5 | 4.1 | 1.3 |
| Branch SA:*V* ($m^2\,m^{-3}$) | 64.2 | 79.5 | 23.2 | 40.3 |

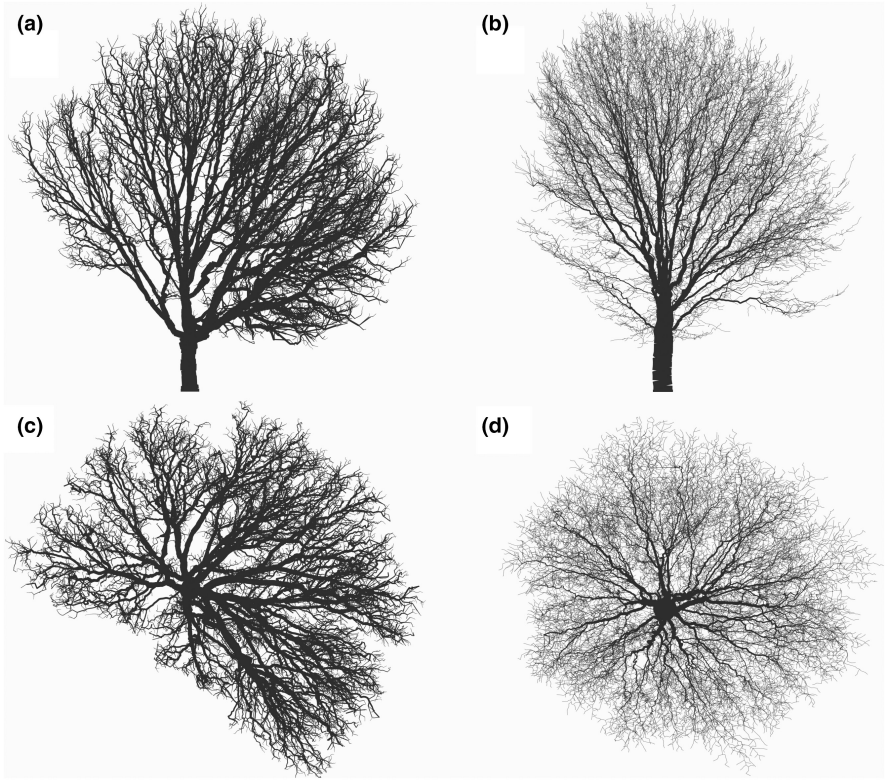


**FIGURE 1** Quantitative structure models showing the vertical profiles of the example study trees, (a) *Celtis occidentalis* L. (common hackberry) and (b) *Ulmus americana* L. (American elm), alongside the horizontal canopy profiles for the (c) hackberry and (d) elm.

a result, a robust codebase exists for creating, storing and analysing graph models, with *NetworkX* (Hagberg et al., 2008) being a notable example. Using the *NetworkX* python library, we represented each QSM in an undirected graph consisting of a collection of nodes connected by edges (Figure 2). The anatomy of these graph models is defined as follows:

- Each *edge* of our graph represents a cylinder (of a tree branch) in the QSM, each node a point in space where two cylinders meet.
- *Edges* are directional, having a start node (or *tail*) and end node (or *tip*).
- One may *traverse* a graph's nodes via edges, evaluating and labeling edges in sequence. A set rules for choosing each subsequent node is referred to as a *traversal algorithm*.
- While traversing a graph, a given edge only allows traversal from its tail (starting node) to its tip (end node).
- A component of a graph is an unordered subset of its nodes and edges.
- We define a *drip node* as a node that has no out-edges (that is not the tail of some edge).

## 2.3 | Graph model approach and interpretation

Each edge of our graph is said to generate an amount of flow proportional to the area of its corresponding cylinder. One can imagine these flows traversing a tree-graph, taking any available in-flow edge, mingling with each other on increasingly shared paths before arriving at a node with no out-edges, eventually dripping to the ground and contributing to throughfall or arriving at a stem-node and flowing down to the root-node. This is the basis for a traversal algorithm that may be used to identify the stemflow and throughfall contributing portions of the canopy; as defined by path and multi-path components. In this way, we may identify: (i) subgraphs containing edges that correspond to either stemflow generating branches or throughfall generating branches and (ii) points on branches in space where excess precipitation falls to the ground. When using our 'branch pruning' algorithm (described below) to define subgraphs of our model and identify these components (Figure 2), the characteristics of each tree graph are combined with assumptions about the behaviour of water intercepted by the tree. These assumptions are as follows:

- Water droplets intercepted by a given section of a tree are assumed to travel toward the stem unless a section with a ≥10° slope away from the stem (i.e. ≤−10°) is encountered. The corresponding edges in our graph model are hereafter referred to as 'drip edges'. The direction of these edges is accordingly directed away from the stem, with their tip defined as a drip node.
- When a flow, consisting of water intercepted by a set of branches, reaches a node with no out-edges, all of the water in said flow is assumed to fall directly to the ground without being intercepted by other sections of the tree.
- The tree's surface is assumed to be fully saturated so that no flow volume is lost due to water absorbed by the bark. Therefore, intercepted water is only lost through dripping to become throughfall.

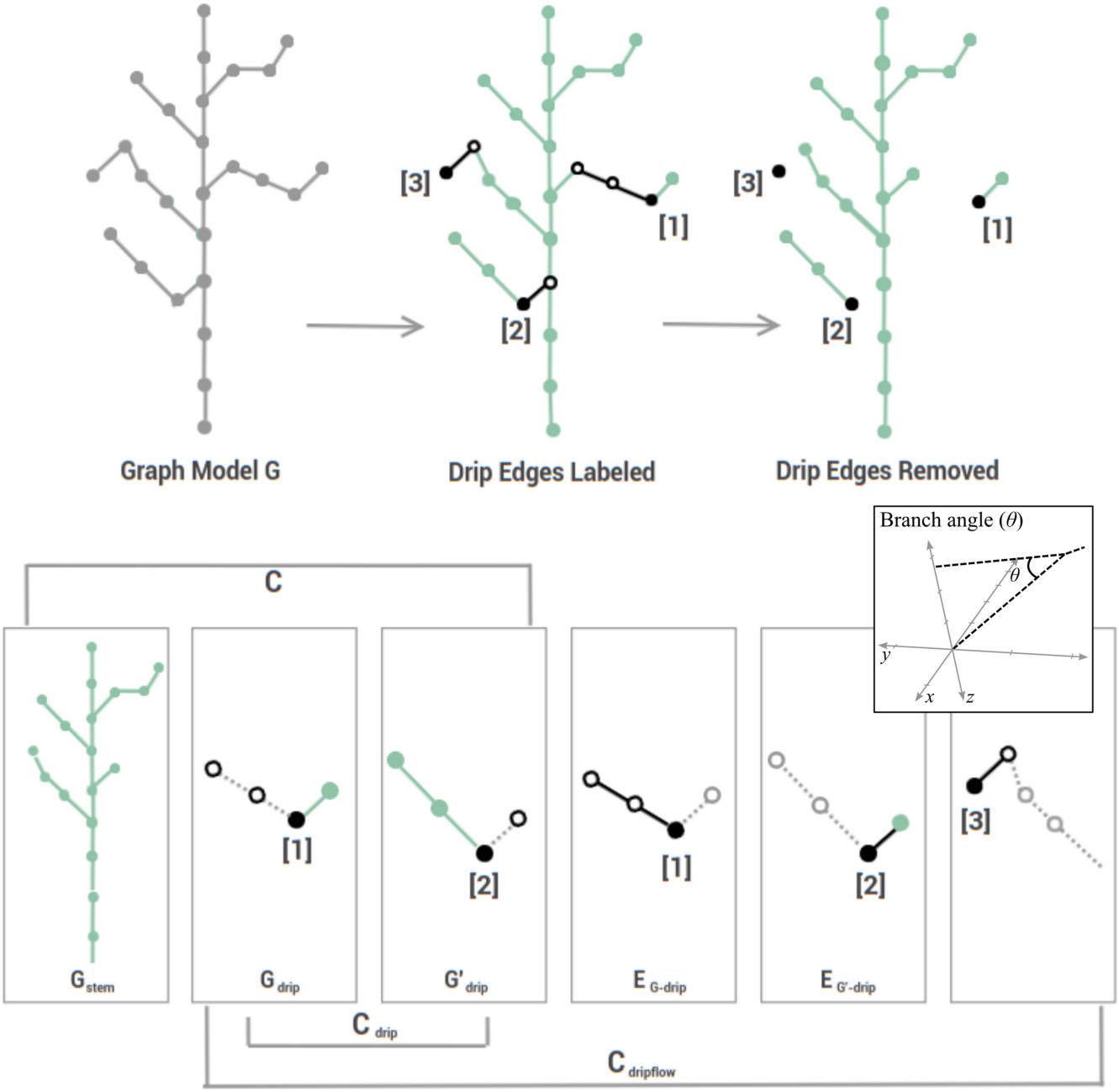


FIGURE 2 Conceptual schematic demonstrating the pruning operation employed here to delineate stemflow and dripflow components in a tree graph model, *G*. An inset is provided showing the angle used for analysis.

- The tree stem (whose corresponding edges may be referred to as the stem of the graph) is assumed to consist entirely of non-drip edges.
- The root node of our graph is the unique stem node in a tree graph with no out-edges.

Under these assumptions, water intercepted by its corresponding branch has a changing flow direction dependent first on the slope of its edge (*e*), and then of the branches it encounters on its path to the stem. For a given *e* this slope ($m_e$) is calculated as shown in Equation (1) below

$$m_e = \frac{(z_1 - z_0)}{\sqrt{(x_1 - x_2)^2 - (y_1 - y_2)^2}}. \quad (1)$$

By defining edge slope in this manner, edges with $m_e \leq 10$, though not necessarily drip edges, correspond to branches which angle downward away from the stem component (i.e. toward the branch tip), while the opposite is true for edges with a positive slope. Each edge of the graph model is then assigned a direction and categorised as having 'out-flow' if it is a drip edge and 'in-flow' otherwise. The cut-off angle above which edges are considered to

have in-flow is configurable and may be selected based on an observational or theoretical justification. As the authors are unaware of past work reporting observed cut-off angles for branchflows, a cut-off angle was experimentally determined from lab simulations on branch analogues (wooden dowels) of diameters representative of a range of tree QSMs (Bhatt & Van Stan, 2022). Briefly, Bhatt and Van Stan (2022) found that applied water flows (100 mL $min^{-1}$) remained attached to the dowels, across a diameter range of 8–51 mm, without dripping until −10°. This cut-off angle has been adopted for the method's application as detailed in subsequent sections. To aid users in assessing theoretical justifications in the absence of observational branchflow data, the code was used for a sensitivity analysis (also to be described and demonstrated in the following section).

## 2.4 | Algorithm for identifying graph models of stemflow and throughfall 'dripflow' components

Let $G$ be the complete digraph model for a given tree (Figure 2). Our assumptions regarding the behaviour of intercepted rainwater imply that the flow generated by an edge of $G$ will traverse $G$ in the direction of its edges until it either encounters a drip node or a stem node. To this end, we consider the subgraph $G_{in}$ of our graph model which consists of only non-drip edges. By assumption, all the edges corresponding to sections of the tree's stem have in-flow and, therefore, all stem edges lie in the same component of $G_{in}$. Likewise, if a path of only inflow edges can be drawn from some non-stem edge to these stem edges, then said edge lies in this same connected component. The component containing the stem edges and all the other edges connected to them via paths with only inflow is defined as $G_{stem}$. Any edge in $G_{in}$ that is not in $G_{stem}$ must be separated from $G_{stem}$ via one or more branch edges with outflow. In this way, only flow generated by edges in $G_{stem}$ contributes to stemflow; thus, the edges of $G_{stem}$ correspond to the complete stemflow generating area of the tree. Edges that are not in $G_{stem}$ contribute to throughfall, falling to the ground at some drip node. Figure 2 illustrates that a tree may have many such drip nodes, that each node has some group of edges ($C_{drip}$) draining to it and how these components can be collectively considered some antithesis of $G_{stem}$—therein labelled $G_{drip}$.

The python library, *NetworkX* provides the bulk of the functionality to label all drip edges, a *remove_edges* function to remove drip edges and generate $G_{in}$ and a *connected_components* function finds the connected component $G_{stem}$ in $G_{in}$. From there, the *remove_edges* function identifies $G_{drip}$ by removing edges of $G_{stem}$ from $G$, and the *connected_components* function identifies the subgraphs of $G$ whose edges generate drip throughfall. We use these subgraphs to aggregate the physical characteristics of branches contributing to stemflow and throughfall at each drip node. As this process relies almost entirely on dictionaries and generator functions, a thirty-thousand-cylinder QSM can be processed in <5 min. This leaves room for future work to add functions to quantify the density of the stemflow generating area (in terms of branching frequency), the interception of throughfall by branches vertically aligned with drip points and to consider implications of many other graph theoretic metrics to differentiate canopy structures.

A sensitivity analysis was conducted to evaluate variability in our model output given different cut-off angles for branchflow. The model was run for 40 regularly spaced cut-off angles spanning from −1.5 radians up to 1.5 radians (roughly −85° to 85°). This span was chosen because there is little-to-no change in drip point location and stemflow watershed boundaries beyond these points. The sensitivity analysis on the QSMs of two trees (Figure 3) systematically examines the cut-off angle's impact on delineating stemflow watersheds and throughfall drip node areas. The open circles in the figure panels represent the stemflow perimeter length, which remains relatively consistent until a sharp decline beyond the experimentally derived cut-off grade (−10°), indicated by a vertical line. Concurrently, the mean contributing surface area for throughfall drip nodes rises with increasing cut-off angles, diminishing in variability near this critical juncture. This point of inflection, observed in *C. occidentalis* (Figure 3a) and *U. americana* (Figure 3b), precedes a significant decrease in stemflow perimeter length and coincides with the plateauing of throughfall drip areas, indicating a shift in the distribution of branch contributing areas at sufficiently large cut-off angles. At this point, large portions of stemflow areas begin to fracture, resulting in drip flows. After a point the canopy becomes dominated by small, low-flow drip points that are inconsistent with field observations except in high intensity rainfall (Van Stan, Hildebrandt, et al., 2020).

Moreover, while a single cut-off angle is applied in the demonstration of the method in the following sections, the overlap in stabilisation (i.e. lower variability) range for the stemflow perimeter and throughfall drip area, which differs between the two example trees (approximately −15° to −10° for *C. occidentalis* vs. −25° to −10° for *U. americana*), suggests the possibility of user discretion in representing diverse conditions. For example, more intense rainfall might call for a steeper branch inclination cut-off, accommodating potential overflow along branches with milder inclinations under different precipitation intensities. Notably, the extent of this range varies with canopy architecture, being broader for *U. americana* (down to −30° in Figure 3b) as opposed to *C. occidentalis*, which stabilises only past −15° (Figure 3a). The differences in this stabilisation range may be a trait itself, describing the sensitivity of stemflow or throughfall responses to increasing rainfall intensity or to bark morphology. Hypothetically, smooth bark may facilitate greater branchflows at shallower angles, while rougher bark might disrupt branchflows at comparatively steeper angles (sensu, Van Stan & Levia, 2010).

The Code and Data Accessibility Statement contains a link to the GitHub repository where the code for this algorithm is stored, as well as a link where the data used to create and evaluate this model has been made publicly available.

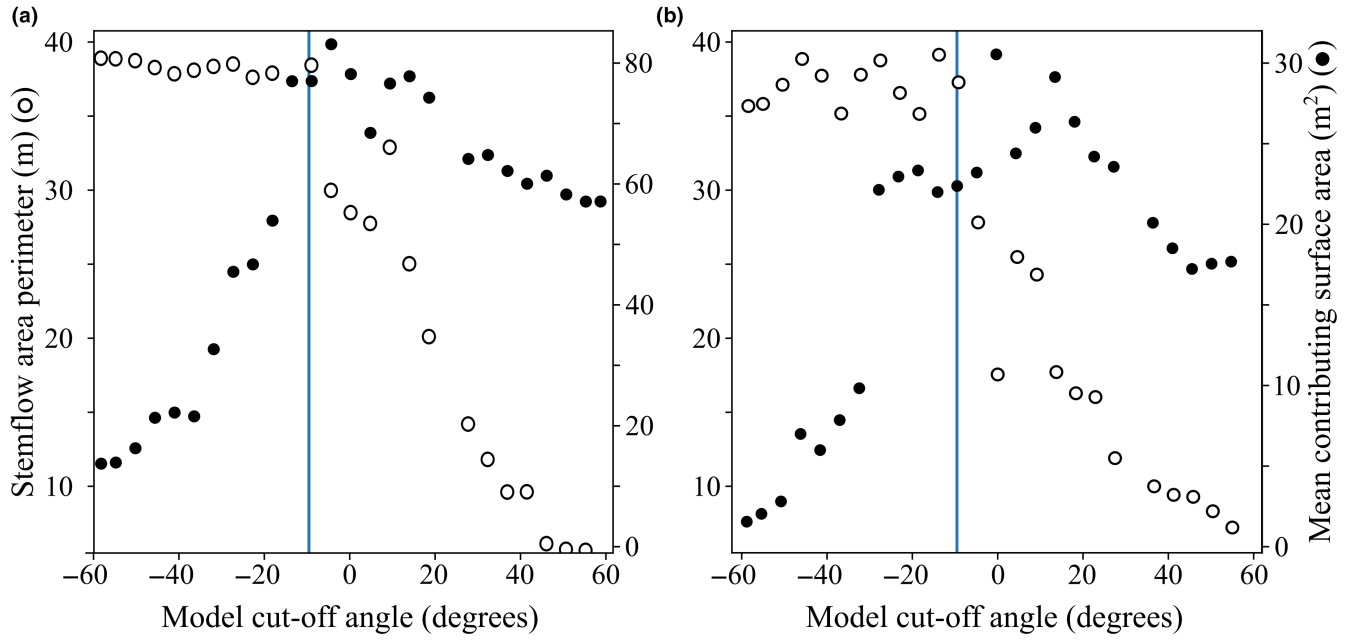


FIGURE 3 Scatterplots showing results from a sensitivity analysis for the cut-off grade within the stemflow and throughfall delineation algorithm, applied to two tree models: (a) *Celtis occidentalis* and (b) *Ulmus americana*. The analysis tracks the stability and subsequent decline of stemflow perimeter length (open circles) as the cut-off angle increases, with a notable decrease occurring beyond −10°. Concurrently, the mean contributing surface area to throughfall drip nodes, shown by filled circles, escalates with wider cut-off angles and plateaus near the same −10° threshold. This plateau signifies a state where the increase in contributing throughfall areas stabilises, illustrating the algorithm's capability to identify a cut-off angle that optimises the demarcation between branches affecting stemflow and throughfall. Example outputs below and above the cut-off angle selected for our demonstration are provided in Figure S1 (stemflow areas and throughfall drip maps).

### 2.5 | Traits derived from graph models of whole canopy, stemflow and dripflow

Ten branch traits commonly hypothesised to influence water flux variations in throughfall and stemflow (Levia et al., 2017; Levia & Germer, 2015; Parker, 1983; Sadeghi et al., 2020) were extracted from this algorithm's results. (1) 2D projected canopy area and (2) diameter at breast height (DBH) were calculated to measure tree size. The 2D projected areas for the (3) stemflow-contributing branch component—'stemflow watershed'—and (4) branch component contributing to throughfall drip points—'dripflow watersheds' are also reported. Alpha shapes were used to provide precision-enhanced boundaries around these watersheds (Edelsbrunner et al., 1983). This method, long used in fluid dynamics (Weatherill, 1992), defines a convex hull representing the area it covers. Here, a curvature (alpha value) of 2.2 was chosen to return the tightest possible, still contiguous boundary. Within these 2D projected areas, we calculated each cylinder's woody (5) surface area, (6) volume, (7) radius and (8) angle. Woody surface area was calculated as the 3D surface area, excluding the top and bottom circular areas of each cylinder as the end-areas of adjoining cylinders do not represent a branch surface. The (9) ratio of woody surface area-to-volume (SA:V) and (10) woody area index (WAI) were also reported. WAI was estimated as half of the 3D surface area of all branches per unit of horizontal ground surface area. Descriptive statistics and histograms were computed for each component.

## 3 | EXAMPLE APPLICATION: A TALE OF TWO TREES

### 3.1 | Canopy trait extraction

To illustrate how refined drainage area boundaries may yield insights into stemflow and throughfall, we compare two trees. The following example serves solely as a semi-quantitative exploration of the method's application to explore common hypotheses, without any intention to quantitatively analyse or specify statistical relationships between the mentioned variables. These trees are (i) within close proximity to each other and (ii) have no neighbour tree near enough to limit their canopy's access to rainfall. Both have similar 'size' traits, with their diameter at breast height (DBH) being ~30 cm, total projected canopy areas being 89 versus 82 $m^2$ $tree^{-1}$, and heights being 12.2 versus 12.3 m (Table 1). A common hypothesis posits that greater tree size corresponds to increased rainwater capture area, and thus, more stemflow (Aboal et al., 1999; André et al., 2008; Van Stan, Hildebrandt, et al., 2020; Van Stan & Levia, 2010; Zimmermann et al., 2015). Despite similar DBH and projected canopy areas, stemflow from these trees over 34 storms was markedly different. Median stemflow volumes from *C. occidentalis* were 2.7 L $event^{-1}$ (interquartile range of 1.5–6.8), resulting in stemflow yields <1% of rainfall across its canopy area. In contrast, *U. americana* median (IQR) stemflow volumes were much greater, 24.0 L $event^{-1}$ (5.3–58.5), generally accounting for yields ~5% (Lewis et al., 2022). Given that only

select branches contribute to stemflow (i.e. the stemflow watershed) (Figure 4), size metrics and total canopy area measures are unlikely to provide insight into the observed stemflow disparities.

The projected area of the alpha shape enclosing the stemflow watershed for both trees represented a similar fraction of the total projected canopy area: 49% (Table 1; Figure 4a,b). Variability in stemflow-contributing area among individual trees has been hypothesised to exert a major influence over stemflow generation (Herwitz, 1986; Levia et al., 2011); this hypothesis is also not supported in this tale of two trees.

Another longstanding hypothesis proposes that branch angle affects stemflow generation (Riegler, 1881). But our model reveals nearly identical branch angle distributions between both trees (Figure 4c). In contrast, an analysis of branch projected area metrics (Table 1), and branch diameter distributions within the stemflow watershed reveals notable differences between the two trees (Figure 4d). Due to *U. americana*'s smaller branch diameters (Figure 4d), this tree had nearly double the surface area-to-volume ratio ($40.3\,m^2\,m^{-3}$) compared to *C. occidentalis* ($23.2\,m^2\,m^{-3}$).

Thus, the greater surface area relative to branch volume within *U. americana*'s stemflow watershed, despite having similar projected area fractions, may allow this tree to capture greater rainfall and to more efficiently channel rainwater to the stem compared to *C. occidentalis*. This hypothesis requires testing with a broader dataset.

Delineating stemflow watersheds within canopies facilitates more robust estimates of stemflow yields and fractions, and assists in standardising stemflow measurements, depending on the research focus. Stemflow yield ($L\,m^{-2}$ tree$^{-1}$, or mm) is typically calculated by dividing volume by the total projected canopy area. Researchers have explored other surface area variables to normalise stemflow volumes, accommodating different perspectives (Allen & Van Stan, 2021; Carlyle-Moses et al., 2020; Van Stan & Allen, 2020). Some standardisations focus on stemflow as a soil input, using variables like the stem base area (Herwitz, 1986) or the potential infiltration area of stemflow rivulets (Carlyle-Moses et al., 2018). The modelled stemflow watershed projected area may more accurately calculate yields, connecting stemflow to its canopy drainage area, like the watershed-stream discharge concept. This may help address concerns about the under-representation of stemflow due to its modest rainfall fractions in many forests (Carlyle-Moses et al., 2018, 2020; Van Stan & Gordon, 2018). The stemflow yields from our two study trees doubled when using the stemflow watershed's projected area. *Ulmus americana*'s stemflow fractions rose from 1%–5% to 2%–9% using this method, with peaks of 13% for most storms >15 mm. However, the interquartile range for stemflow fraction from *C. occidentalis* was <1% whether applying the stemflow watershed area (0.2%–0.7%) or the total canopy projected area (0.1%–0.3%).

The number of throughfall drip nodes was 3000–4000 per tree but was greater for *U. americana* than *C. occidentalis* (Table 2). Note that variability in the number of drip nodes and their location within the canopy may be seen in the supplemental materials (Figure S1). Some drip nodes amass rainwater from a small component of the branch network and thus are not traditionally defined 'drip points': spots experiencing more throughfall per unit area than open rainfall (Keim & Link, 2018; Van Stan, Hildebrandt, et al., 2020). In the algorithm, users may determine which 'drip points' refer to 'drip nodes' by setting a threshold in contribution area—for example, Figure 5 plots the throughfall drip points when the threshold is set to the 98th percentile of all drip nodes. In this

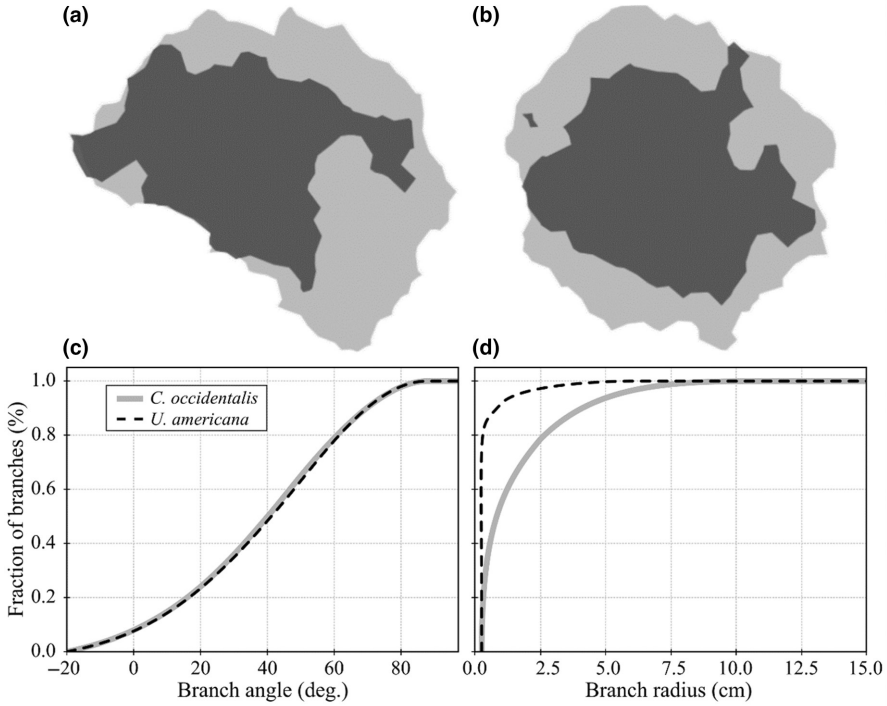


**FIGURE 4** Comparison of the total projected canopy area (light grey) and the projected stemflow-contributing branch area (dark grey) for (a) *Celtis occidentalis* L. (common hackberry) and (b) *Ulmus americana* L. (American elm). The areas shown in panels (a and b) are reported in Table 1. In the stemflow watershed, the distribution of (c) branch angles was nearly identical; however, (d) the branch radii distribution obviously differ.

**TABLE 2** Traits for all drip nodes in the canopy and for the drip points (representing the top 98th percentile of projected drip-related drainage area).

| | All drip nodes (>0.001 $m^2$) | | Drip points (>98th percentile) | |
|---|---|---|---|---|
| **Traits** | *C. occidentalis* | *U. americana* | *C. occidentalis* | *U. americana* |
| Number (*n*) | 3128 | 4253 | 69 | 94 |
| Projected branch area ($m^2$) | 64.2 | 20.4 | 28.6 | 7.8 |
| Branch volume (*V*, $m^3$) | 4.62 | 0.47 | 1.57 | 0.15 |
| Branch surface area (SA, $m^2$) | 214.3 | 77.6 | 87.1 | 30.4 |
| Branch SA:*V* ($m^2 m^{-3}$) | 46.4 | 165.2 | 20.7 | 202.5 |

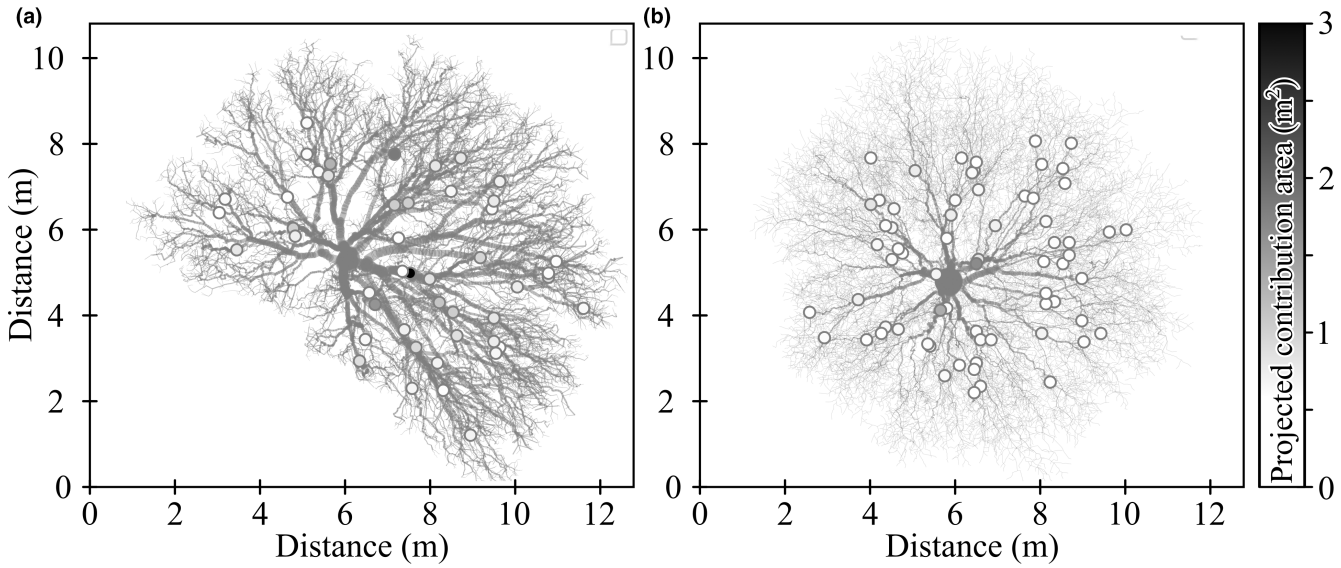


**FIGURE 5** Panels showing drip point maps for (a) *Celtis occidentalis* L. (common hackberry) and (b) *Ulmus americana* L. (American elm), where the shade of each dot indicates the amount of contributing projected branch area. Plotted drip points are the top 98th percentile of all drip nodes.

example, distinctive throughfall redistribution patterns are apparent for *C. occidentalis* (Figure 5a) and *U. americana* (Figure 5b). Interestingly, *U. americana*, with higher stemflow and has more and smaller (contributing projected area) drip points than *C. occidentalis* (Figure 5; Table 2). This difference potentially suggests an intrinsic variation in water drainage between the trees. The reduced stemflow in *C. occidentalis* suggests that more water shedding must occur at drip points.

Maps like Figure 5a,b (and Figure S1), if validated across diverse sites and storms, could guide throughfall monitoring network design. Throughfall patterns are difficult to effectively monitor using funnels or troughs at reasonable labour and costs (Van Stan, Hildebrandt, et al., 2020; Zimmermann et al., 2010, 2016) and throughfall sampling efforts often fall short of the theoretical optimum protocols suggested (see Voss et al., 2016; Zimmermann et al., 2010, 2016; Zimmermann & Zimmermann, 2014). *Ex-ante* human inference regarding these patterns (i.e. where drip and dry spots may occur) is currently unfeasible. Yet, knowing potential (modelled) drip points might enable optimal sampling with fewer gauges. If these maps align with field observations, they may help explore how throughfall affects soil moisture and biogeochemistry—a significant knowledge gap (Coenders-Gerrits et al., 2013; Fischer-Bedtke et al., 2023; Ma et al., 2014).

## 4 | LIMITATIONS OF THE CURRENT MODEL

Our current model bears limitations. First, it uses leafless scan data, overlooking the impact of leaves on stemflow and throughfall patterns. While leaves generally shield branches from rainfall, seasonally decreasing stemflow (Herbst et al., 2008; Pypker et al., 2011), it is conceivable that inclined leaves may also channel rainwater toward branches. Relevant contributions of rainwater to stemflow, however, is rarely reported (Biddick et al., 2018). Still, leaf contributions to the boundaries and projected areas of stemflow (and to a lesser extent, drip) watersheds is likely to be minimal, as leaves add a few square centimetres to the overall $10^0$–$10^1$ $m^2$ projected area enclosing these branch components. Second, analysing evergreen trees introduces another challenge. Although algorithms can distinguish between leaves and wood in the lidar data (Stovall et al., 2021), such workflows have limitations (e.g. the most distal, thin branches will not be well resolved). Third, our model depends on another underlying algorithm, the SimpleForest algorithm that converts lidar point clouds to canopy QSMs. This implies that the potential variability in derived cylinder models from different scans or interpretations of the same

tree requires careful consideration of model representativeness. Despite meticulous planning, occlusion remains an inherent challenge in terrestrial lidar scanning (Mathes et al., 2023), yet our methodology minimises its impact, ensuring a high degree of accuracy in our tree models. Finally, though scanning every individual tree is not feasible, our method forms a base for scalable models. For example, data-driven (i.e. machine learning) models could be trained to map remotely sensed observations (e.g. crown diameter, canopy height and land cover class) to effective canopy area metrics derived from our method. Therefore, if adequately sampled, the outputs from our method could be harnessed to create predictive models for effective canopy areas, optimising the model's utility in broader canopy precipitation partitioning research. Despite the model's insights, its constraints underscore the importance of adapting and refining the approach across diverse tree species and conditions.

## 5 | CONCLUSIONS

This study presents a graph theoretic model, derived from terrestrial lidar scanning, to delineate branch drainage areas for stemflow and throughfall in isolated tree canopies. Addressing the current gap in defining mechanistic boundaries for throughfall and stemflow research, our model provides enhanced insights, especially evident in the comparative study of *Celtis occidentalis* and *Ulmus americana*—trees with similar size but varying canopy architecture and stemflow outputs and throughfall drip patterns. Our findings suggest that the commonly-applied boundary for stemflow research, total projected canopy area, likely includes a substantial number and area of non-contributing branches. Our model enables refined understanding of the stemflow-contributing area within canopies, potentially allowing for more accurate and robust estimates of stemflow yields and fractions. It further outlines the spatial variability in throughfall drip points (and potential volumes) that would be expected to be derived from branch traits (e.g. angles and diameters) that are known to be highly variable within and between different tree canopies. Thus, we expect application of our graph theoretic model will improve throughfall monitoring techniques and mechanistic studies of throughfall variation. When substantiated by comprehensive field studies across diverse trees and environments, this model can bridge knowledge deficits, especially linking throughfall, stemflow, and the cycling of water and elements in soil. Thus, we encourage the research community to utilise our open-source model and contribute to our Zenodo repository. This endeavour may revolutionise hydrometeorological studies and provide a foundation for the development of informed conservation strategies grounded in nuanced knowledge of canopy trait-specific hydrological processes.

### AUTHOR CONTRIBUTIONS

Collin Wischmeyer and John Van Stan II conceived the ideas and designed methodology in collaboration with Travis E. Swanson and Kevin E. Mueller; Kevin E. Mueller coordinated the fieldwork at Secrest; Nicholas R. Lewis and Jillian Bastock collected the lidar data; Collin Wischmeyer analysed the data under advisement by John T. Van Stan and Travis E. Swanson; Collin Wischmeyer and John Van Stan II led the writing of the manuscript. All authors contributed critically to the drafts and gave final approval for publication.

### ACKNOWLEDGEMENTS

The authors gratefully acknowledge the support of US-NSF DEB-2213623, the staff at Secrest Arboretum, including Jason Veil, Paul Snyder and Roger Hamilton, as well as Sarah Blair for initiating the study of rainfall partitioning of the two focal trees.

### CONFLICT OF INTEREST STATEMENT

The authors have no conflict of interest to declare.

### PEER REVIEW

The peer review history for this article is available at https://www.webofscience.com/api/gateway/wos/peer-review/10.1111/2041-210X.14378.

### DATA AVAILABILITY STATEMENT

Code and data can be found in the following GitHub link https://github.com/wischmcj/canopyHydrodynamics. Raw data is archived at https://zenodo.org/records/11513597 (Van Stan et al., 2024a) and the model outputs underlying the figures and sensitivity analyses are archived at https://zenodo.org/records/11513047 (Van Stan et al., 2024b).

### ORCID

*Kevin E. Mueller* https://orcid.org/0000-0002-0739-7472
*John T. Van Stan II* https://orcid.org/0000-0002-0692-7064

### REFERENCES

Aboal, J. R., Morales, D., Hernández, M., & Jiménez, M. S. (1999). The measurement and modelling of the variation of stemflow in a laurel forest in Tenerife, Canary Islands. *Journal of Hydrology*, *221*(3–4), 161–175.

Allen, S. T., & Van Stan, J. T. (2021). Response: Commentary: What we know about Stemflow's infiltration area. *Frontiers in Forests and Global Change*, *4*. https://doi.org/10.3389/ffgc.2021.639511

André, F., Jonard, M., & Ponette, Q. (2008). Influence of species and rain event characteristics on stemflow volume in a temperate mixed oak-beech stand. *Hydrological Processes*, *22*(22), 4455–4466. https://doi.org/10.1002/hyp.7048

Atkins, J. W., Bohrer, G., Fahey, R. T., Hardiman, B. S., Morin, T. H., Stovall, A. E. L., Zimmerman, N., & Gough, C. M. (2018). Quantifying vegetation and canopy structural complexity from terrestrial LiDAR data using the FORESTR R package. *Methods in Ecology and Evolution*, *9*(10), 2057–2066.

Aubrey, D. P. (2020). Relevance of precipitation partitioning to the tree water and nutrient balance. In J. T. Van Stan, E. D. Gutmann, & J. Friesen (Eds.), *Precipitation partitioning by vegetation* (pp. 147–162). Springer. https://doi.org/10.1007/978-3-030-29702-2_10

Bhatt, B., & Van Stan, J. T. (2022). *H12A-0043: Simulating branchflows to investigate the range of flow rates in canopies and their contribution to stemflow*. American Geophysical Union Fall Meeting.

Biddick, M., Hutton, I., & Burns, K. C. (2018). An alternative water transport system in land plants. *Proceedings of the Royal Society B: Biological Sciences*, *285*(1884), 20180995.

Brede, B., Terryn, L., Barbier, N., Bartholomeus, H. M., Bartolo, R., Calders, K., Derroire, G., Krishna Moorthy, S. M., Lau, A., Levick, S. R., Raumonen, P., Verbeeck, H., Di Wang, T. W., van der Zee, J., & Herold, M. (2022). Non-destructive estimation of individual tree biomass: Allometric models, terrestrial and UAV laser scanning. *Remote Sensing of Environment*, *280*, 113180.

Calders, K., Adams, J., Armston, J., Bartholomeus, H., Bauwens, S., Bentley, L. P., Chave, J., Danson, F. M., Demol, M., Disney, M., Gaulton, R., Krishna Moorthy, S. M., Levick, S. R., Saarinen, N., Schaaf, C., Stovall, A., Terryn, L., Wilkes, P., & Verbeeck, H. (2020). Terrestrial laser scanning in forest ecology: Expanding the horizon. *Remote Sensing of Environment*, *251*, 112102. https://doi.org/10.1016/j.rse.2020.112102

Carlyle-Moses, D. E., Iida, S., Germer, S., Llorens, P., Michalzik, B., Nanko, K., Tanaka, T., Tischer, A., & Levia, D. F. (2020). Commentary: What we know about Stemflow's infiltration area. *Frontiers in Forests and Global Change*, *3*. https://doi.org/10.3389/ffgc.2020.577247

Carlyle-Moses, D. E., Iida, S., Germer, S., Llorens, P., Michalzik, B., Nanko, K., Tischer, A., & Levia, D. F. (2018). Expressing stemflow commensurate with its ecohydrological importance. *Advances in Water Resources*, *121*, 472–479.

Cavelier, J., Jaramillo, M., Solis, D., & de León, D. (1997). Water balance and nutrient inputs in bulk precipitation in tropical montane cloud forest in Panama. *Journal of Hydrology*, *193*(1–4), 83–96.

Cayley, A. (1857). On the theory of the analytical forms called trees. *Philosophical Magazine*, *4*(13), 172–176.

Coenders-Gerrits, A. M. J., Hopp, L., Savenije, H. H. G., & Pfister, L. (2013). The effect of spatial throughfall patterns on soil moisture patterns at the hillslope scale. *Hydrology and Earth System Sciences*, *17*(5), 1749–1763.

Coenders-Gerrits, A. M. J., Schilperoort, B., & Jiménez-Rodríguez, C. (2020). Evaporative processes on vegetation: An inside look. In J. T. Van Stan, E. D. Gutmann, & J. Friesen (Eds.), *Precipitation partitioning by vegetation: A global synthesis* (pp. 35–48). Springer Nature. https://doi.org/10.1007/978-3-030-29702-2_3

Dalton, J. (1802). Experiments and observations to determine whether the quantity of rain and dew is equal to the quantity of water carried off by the rivers and raised by evaporation; with an enquiry into the origin of springs. *Proceedings of the Manchester Literary and Philosophical Society*, *5*(2), 346–372.

Dassot, M., Constant, T., & Fournier, M. (2011). The use of terrestrial LiDAR technology in forest science: Application fields, benefits and challenges. *Annals of Forest Science*, *68*(5), 959–974. https://doi.org/10.1007/s13595-011-0102-2

Disney, M. (2019). Terrestrial LiDAR: A three-dimensional revolution in how we look at trees. *New Phytologist*, *222*(4), 1736–1741. https://doi.org/10.1111/nph.15517

Druschke, C. G. (2018). Watershed as common-place. In *Readings in rhetorical fieldwork* (pp. 357–370). Routledge. https://doi.org/10.4324/9781351190473-26

Dunkerley, D. (2020). A review of the effects of throughfall and stemflow on soil properties and soil erosion. In J. T. Van Stan, E. D. Gutmann, & J. Friesen (Eds.), *Precipitation partitioning by vegetation: A global synthesis* (pp. 183–214). Springer Nature. https://doi.org/10.1007/978-3-030-29702-2_12

Edelsbrunner, H., Kirkpatrick, D., & Seidel, R. (1983). On the shape of a set of points in the plane. *IEEE Transactions on Information Theory*, *29*(4), 551–559. https://doi.org/10.1109/TIT.1983.1056714

Fischer-Bedtke, C., Metzger, J. C., Demir, G., Wutzler, T., & Hildebrandt, A. (2023). Throughfall spatial patterns translate into spatial patterns of soil moisture dynamics—Empirical evidence. *Hydrology and Earth System Sciences*, *27*(15), 2899–2918. https://doi.org/10.5194/hess-27-2899-2023

Fortin, J.-P., Turcotte, R., Massicotte, S., Moussa, R., Fitzback, J., & Villeneuve, J.-P. (2001). Distributed watershed model compatible with remote sensing and GIS data. I: Description of model. *Journal of Hydrologic Engineering*, *6*(2), 91–99. https://doi.org/10.1061/(ASCE)1084-0699(2001)6:2(91)

Friesen, J. (2020). Flow pathways of throughfall and stemflow through the subsurface. In J. T. Van Stan, E. D. Gutmann, & J. Friesen (Eds.), *Precipitation partitioning by vegetation: A global synthesis* (pp. 215–228). Springer Nature. https://doi.org/10.1007/978-3-030-29702-2_13

Gotsch, S. G., Draguljić, D., & Williams, C. J. (2018). Evaluating the effectiveness of urban trees to mitigate storm water runoff via transpiration and stemflow. *Urban Ecosystems*, *21*(1), 183–195. https://doi.org/10.1007/s11252-017-0693-y

Hackenberg, J., Calders, K., Demol, M., Raumonen, P., Piboule, A., & Disney, M. (2021). SimpleForest—A comprehensive tool for 3d reconstruction of trees from forest plot point clouds. *BioRxiv*, https://doi.org/10.1101/2021.07.29.454344

Hagberg, A. A., Schult, D. A., & Swart, P. J. (2008). Exploring network structure, dynamics, and function using NetworkX. In G. Varoquaux, T. Vaught, & J. Millman (Eds.), *Proceedings of the 7th python in science conference (SciPy2008)* (pp. 11–15). The Open Journal.

Herbst, M., Rosier, P. T. W., McNeil, D. D., Harding, R. J., & Gowing, D. J. (2008). Seasonal variability of interception evaporation from the canopy of a mixed deciduous forest. *Agricultural and Forest Meteorology*, *148*(11), 1655–1667. https://doi.org/10.1016/j.agrformet.2008.05.011

Herwitz, S. R. (1986). Infiltration-excess caused by stemflow in a cyclone-prone tropical rainforest. *Earth Surface Processes and Landforms*, *11*(4), 401–412.

Jeziorska, J. (2019). UAS for wetland mapping and hydrological modeling. *Remote Sensing*, *11*(17), 1997. https://doi.org/10.3390/rs11171997

Ji, S., Omar, S. I., Zhang, S., Wang, T., Chen, C., & Zhang, W. (2022). Comprehensive evaluation of throughfall erosion in the banana plantation. *Earth Surface Processes and Landforms*, *47*(12), 2941–2949. https://doi.org/10.1002/esp.5435

Keim, R. F., & Link, T. E. (2018). Linked spatial variability of throughfall amount and intensity during rainfall in a coniferous forest. *Agricultural and Forest Meteorology*, *248*, 15–21.

Klamerus-Iwan, A., Link, T. E., Keim, R. F., & Van Stan, J. T. (2020). Storage and routing of precipitation through canopies. In J. T. Van Stan, E. D. Gutmann, & J. Friesen (Eds.), *Precipitation partitioning by vegetation: A global synthesis* (pp. 17–34). Springer Nature. https://doi.org/10.1007/978-3-030-29702-2_2

Lau, A., Bentley, L. P., Martius, C., Shenkin, A., Bartholomeus, H., Raumonen, P., Malhi, Y., Jackson, T., & Herold, M. (2018). Quantifying branch architecture of tropical trees using terrestrial LiDAR and 3D modelling. *Trees*, *32*, 1219–1231.

Levia, D. F., & Frost, E. E. (2006). Variability of throughfall volume and solute inputs in wooded ecosystems. *Progress in Physical Geography*, *30*(5), 605–632. https://doi.org/10.1177/0309133306071145

Levia, D. F., & Germer, S. (2015). A review of stemflow generation dynamics and stemflow-environment interactions in forests and shrublands. *Reviews of Geophysics*, *53*(3), 673–714.

Levia, D. F., Hudson, S. A., Llorens, P., & Nanko, K. (2017). Throughfall drop size distributions: A review and prospectus for future research. *Wiley Interdisciplinary Reviews: Water*, *4*(4), e1225.

Levia, D. F., Keim, R. F., Carlyle-Moses, D. E., & Frost, E. E. (2011). Throughfall and stemflow in wooded ecosystems. In D. F. Levia, D. E. Carlyle-Moses, & T. Tanaka (Eds.), *Forest hydrology and biogeochemistry: Synthesis of past research and future directions* (pp. 425–443). Springer. https://doi.org/10.1007/978-94-007-1363-5_21

Lewis, N., Mueller, K., Swanson, T., Blair, S., Bastock, J., & Van Stan, J. (2022). *Flashy trees in flashy watersheds? Storm responses of water*

*drainage (as stemflow) from isolated urban trees (H12A-51)*. American Geophysical Union Fall Meeting.

Ma, Y., Van Dam, R. L., & Jayawickreme, D. H. (2014). Soil moisture variability in a temperate deciduous forest: Insights from electrical resistivity and throughfall data. *Environmental Earth Sciences*, *72*(5), 1367–1381. https://doi.org/10.1007/s12665-014-3362-y

Mathes, T., Seidel, D., Häberle, K. H., Pretzsch, H., & Annighöfer, P. (2023). What are we missing? Occlusion in laser scanning point clouds and its impact on the detection of single-tree morphologies and stand structural variables. *Remote Sensing*, *15*(2), 450.

Parker, G. G. (1983). Throughfall and stemflow in the forest nutrient cycle. *Advances in Ecological Research*, *13*, 57–133. https://doi.org/10.1016/S0065-2504(08)60108-7

Peel, M. C., & McMahon, T. A. (2020). Historical development of rainfall-runoff modeling. *WIREs Water*, *7*(5). https://doi.org/10.1002/wat2.1471

Phillips, J. D., Schwanghart, W., & Heckmann, T. (2015). Graph theory in the geosciences. *Earth-Science Reviews*, *143*, 147–160. https://doi.org/10.1016/j.earscirev.2015.02.002

Pypker, T. G., Levia, D. F., Staelens, J., & Van Stan, J. T. (2011). Canopy structure in relation to hydrological and biogeochemical fluxes. In *Forest hydrology and biogeochemistry* (pp. 371–388). Springer. https://doi.org/10.1007/978-94-007-1363-5_18

Qin, H., Zhou, W., Yao, Y., & Wang, W. (2022). Individual tree segmentation and tree species classification in subtropical broadleaf forests using UAV-based LiDAR, hyperspectral, and ultrahigh-resolution RGB data. *Remote Sensing of Environment*, *280*, 113143. https://doi.org/10.1016/j.rse.2022.113143

Qualls, R. G. (2020). Role of precipitation partitioning in litter biogeochemistry. In J. T. Van Stan, E. D. Gutmann, & J. Friesen (Eds.), *Precipitation partitioning by vegetation* (pp. 163–182). Springer Nature. https://doi.org/10.1007/978-3-030-29702-2_11

Reitberger, J., Schnörr, C., Krzystek, P., & Stilla, U. (2009). 3D segmentation of single trees exploiting full waveform LIDAR data. *ISPRS Journal of Photogrammetry and Remote Sensing*, *64*(6), 561–574. https://doi.org/10.1016/j.isprsjprs.2009.04.002

Riegler, W. (1881). Beobachtungen über die Abfuhr meteorischen Wassers entlang den Hochstämmen. *Mitteilungen Der Forstlichen Bundes-Versuchsanstalt Wien*, *2*, 234–246.

Sadeghi, S. M. M., Gordon, A. G., & Van Stan, J. T. (2020). A global synthesis of throughfall and stemflow hydrometeorology. In J. T. Van Stan, E. D. Gutmann, & J. Friesen (Eds.), *Precipitation partitioning by vegetation: A global synthesis* (pp. 49–70). Springer Nature. https://doi.org/10.1007/978-3-030-29702-2_4

Shuttleworth, W. J. (1989). Micrometeorology of temperate and tropical forest. *Philosophical Transactions of the Royal Society of London. B, Biological Sciences*, *324*(1223), 299–334.

Smith, C. T. (2019). The Drainage Basin as an historical basis for human activity. In *Introduction to geographical hydrology* (pp. 20–29). Routledge. https://doi.org/10.4324/9780429273322-3

Stovall, A. E. L., Masters, B., Fatoyinbo, L., & Yang, X. (2021). TLSL eAF: Automatic leaf angle estimates from single-scan terrestrial laser scanning. *New Phytologist*, *232*(4), 1876–1892. https://doi.org/10.1111/nph.17548

Stubbins, A., Guillemette, F., & Van Stan, J. T. (2020). Throughfall and stemflow: The crowning headwaters of the aquatic carbon cycle. In J. T. Van Stan, E. D. Gutmann, & J. Friesen (Eds.), *Precipitation partitioning by vegetation: A global synthesis* (pp. 121–132). Springer Nature. https://doi.org/10.1007/978-3-030-29702-2_8

Van Stan, J. T., & Allen, S. T. (2020). What we know about stemflow's infiltration area. *Frontiers in Forests and Global Change*, *3*. https://doi.org/10.3389/ffgc.2020.00061

Van Stan, J. T., & Gordon, D. A. (2018). Mini-review: Stemflow as a resource limitation to near-stem soils. *Frontiers in Plant Science*, *9*. https://doi.org/10.3389/fpls.2018.00248

Van Stan, J. T., Hildebrandt, A., Friesen, J., Metzger, J. C., & Yankine, S. A. (2020). Spatial variablity and temporal stability of local net precipitation patterns. In J. T. Van Stan, E. D. Gutmann, & J. Friesen (Eds.), *Precipitation partitioning by vegetation: A global synthesis* (pp. 89–104). Springer Nature. https://doi.org/10.1007/978-3-030-29702-2_6

Van Stan, J. T., & Levia, D. F. (2010). Inter- and intraspecific variation of stemflow production from *Fagus grandifolia* Ehrh. (American beech) and *Liriodendron tulipifera* L. (yellow poplar) in relation to bark microrelief in the eastern United States. *Ecohydrology*, *3*, 11–19. https://doi.org/10.1002/eco.83

Van Stan, J. T., Morris, C. E., Aung, K., Kuzyakov, Y., Magyar, D., Rebollar, E. A., Remus-Emsermann, M. N., Uroz, S., & Vandenkoornhuyse, P. (2020). Precipitation partitioning—Hydrologic highways between microbial communities of the plant microbiome? In J. T. Van Stan, E. D. Gutmann, & J. Friesen (Eds.), *Precipitation partitioning by vegetation: A global synthesis*. Springer Nature. https://doi.org/10.1007/978-3-030-29702-2_14

Van Stan, J. T., & Pinos, J. (2023). Three fundamental challenges to the advancement of stemflow research and its integration into natural science. *Water*, *16*(1), 117. https://doi.org/10.3390/w16010117

Van Stan, J. T., Ponette-González, A. G., Swanson, T., & Weathers, K. C. (2021). Throughfall and stemflow are major hydrologic highways for particulate traffic through tree canopies. *Frontiers in Ecology and the Environment*, *19*(7), 404–410. https://doi.org/10.1002/fee.2360

Van Stan, J. T., Van Stan, J. H., & Levia, D. F. (2014). Meteorological influences on stemflow generation across diameter size classes of two morphologically distinct deciduous species. *International Journal of Biometeorology*, *58*(10), 2059–2069. https://doi.org/10.1007/s00484-014-0807-7

Van Stan, J. T., Wischmeyer, C., Swanson, T., Mueller, K. E., Lewis, N. R., & Bastock, J. (2024a). *Full tree QSMs: LIDAR driven stemflow mapping*. https://zenodo.org/records/11513597

Van Stan, J. T., Wischmeyer, C., Swanson, T., Mueller, K. E., Lewis, N. R., & Bastock, J. (2024b). *Testing data: LIDAR driven stemflow mapping*. https://zenodo.org/records/11513047

Von Bertalanffy, L. (1950). An outline of general system theory. *The British Journal for the Philosophy of Science*, *1*(2), 134–165.

Voss, S., Zimmermann, B., & Zimmermann, A. (2016). Detecting spatial structures in throughfall data: The effect of extent, sample size, sampling design, and variogram estimation method. *Journal of Hydrology*, *540*, 527–537. https://doi.org/10.1016/j.jhydrol.2016.06.042

Weatherill, N. P. (1992). Delaunay triangulation in computational fluid dynamics. *Computers & Mathematics with Applications*, *24*(5–6), 129–150. https://doi.org/10.1016/0898-1221(92)90045-J

Zhang, B., Wdowinski, S., Gann, D., Hong, S.-H., & Sah, J. (2022). Spatiotemporal variations of wetland backscatter: The role of water depth and vegetation characteristics in Sentinel-1 dual-polarization SAR observations. *Remote Sensing of Environment*, *270*, 112864. https://doi.org/10.1016/j.rse.2021.112864

Zhang, H., Levia, D. F., He, B., Wu, H., Liao, A., Carlyle-Moses, D. E., Liu, J., Wang, N., Li, J., & Fu, C. (2020). Interspecific variation in tree- and stand-scale stemflow funneling ratios in a subtropical deciduous forest in eastern China. *Journal of Hydrology*, *590*, 125455. https://doi.org/10.1016/j.jhydrol.2020.125455

Zimmermann, A., Uber, M., Zimmermann, B., & Levia, D. F. (2015). Predictability of stemflow in a species-rich tropical forest. *Hydrological Processes*, *29*(23), 4947–4956. https://doi.org/10.1002/hyp.10554

Zimmermann, A., Voss, S., Metzger, J. C., Hildebrandt, A., & Zimmermann, B. (2016). Capturing heterogeneity: The role of a study area's extent for estimating mean throughfall. *Journal of Hydrology*, *542*, 781–789.

Zimmermann, A., & Zimmermann, B. (2014). Requirements for throughfall monitoring: The roles of temporal scale and canopy complexity. *Agricultural and Forest Meteorology*, *189*, 125–139.

Zimmermann, A., Zimmermann, B., & Elsenbeer, H. (2009). Rainfall redistribution in a tropical forest: Spatial and temporal patterns. *Water Resources Research*, *45*(11). https://doi.org/10.1029/2008wr007470

Zimmermann, B., Zimmermann, A., Lark, R. M., & Elsenbeer, H. (2010). Sampling procedures for throughfall monitoring: A simulation study. *Water Resources Research*, *46*(1). https://doi.org/10.1029/2009wr007776

## SUPPORTING INFORMATION

Additional supporting information can be found online in the Supporting Information section at the end of this article.

**Figure S1:** Algorithm outputs for stemflow areas (dark grey) and drip points (circles with collection area per drip point indicated by circle radius) at varying cut-off angles for *Ulmus americana* (left) and *Celtis occidentalis* (right).

**How to cite this article:** Wischmeyer, C., Swanson, T. E., Mueller, K. E., Lewis, N. R., Bastock, J., & Van Stan, J. T. II (2024). A LiDAR-driven pruning algorithm to delineate canopy drainage areas of stemflow and throughfall drip points. *Methods in Ecology and Evolution*, *00*, 1–13. https://doi.org/10.1111/2041-210X.14378